

# OBSERVATION OF DUST TRAPPING USING VIDEO CAMERAS

Y. Tanimoto<sup>#</sup>, T. Honda, S. Sakanaka, KEK, Tsukuba, Japan

## Abstract

A sudden decrease in beam lifetime is observed sometimes in many electron storage rings. Such an event has been commonly attributed to dust trapping, but its mechanism has not yet been entirely elucidated. Our dust-trapping research at the Photon Factory Advanced Ring (PF-AR) showed that trapped dust under certain conditions can be visually observed by video cameras, and the recorded footage revealed that the trapped dust moved longitudinally. In addition, light emissions from the dust suggested that its temperature reached 1000 K or more. Recently, we have pursued this research using supersensitive cameras and, as a result, trapped dust particles were repeatedly observed. In addition, these new experiments revealed that trapped dust behaved differently under different conditions. Thus, direct observation of trapped dust is becoming an effective way to investigate the dust-trapping mechanism.

## INTRODUCTION

A sudden decrease in beam lifetime, ascribed to the trapping of positively charged dust particles, is an arduous problem in the operation of the PF-AR [1]. In order to investigate this phenomenon, we conducted dust-trapping experiments [2] upon empirical evidence that some of the dust-trapping events were caused by electric discharges in distributed ion pumps (DIPs) and in discharge-prone vacuum chambers, such as in-vacuum insertion devices or strip-line electrodes. The former was caused by applied DC high voltage (HV), and the latter was caused by beam induced RF fields and high-peak electric fields from a single-bunched electron beam.

The aims of this study were twofold: first, to demonstrate that these kinds of discharges can cause dust trapping; and second, to accumulate knowledge toward a further understanding of the dust-trapping mechanism by observing the behavior of the trapped dust.

We employed a device that can intentionally produce the two kinds of electric discharges to simulate the dust sources in the accelerator operation, and installed it in the PF-AR, the main parameters of which are listed in Table 1. In the early stage of the study, the first goal was successfully achieved; the two kinds of intentional discharges were shown capable of repeatedly provoking the dust-trapping phenomenon.

More surprisingly, trapped dust during one dust event was visually observed by standard video cameras. A snapshot from this footage is shown in Fig. 1. The event was triggered by a mechanical movement of an electrode, and the dust seemed to be produced by friction or shock at the electrode because no discharge evidence was observed either by the video cameras or by a Bayard-Alpert gauge

(BAG). The luminous dust moved longitudinally at an estimated speed of 10 m/s or more, and disappeared after 6 s from first appearance, while the dust-trapping event lasted for 15 min (according to gamma-ray detection). The dust diameter estimated from the reduced lifetime [3] (1 h) was about 2  $\mu\text{m}$ , assuming the dust material to be silica. Image analysis suggested that the main process of the light emission from the trapped dust was thermal (blackbody) radiation and the temperature reached 1000 K or more.

Table 1: Principal parameters of PF-AR.

Stored Beam Energy	6.5 GeV
Injection Beam Energy	3.0 GeV
Initial Stored Current	62 mA
Circumference	377 m
Beam Emittance	293 nm $\cdot$ rad
Harmonic Number	640
Number of Bunches	1 (single-bunch)
Beam Lifetime	20-23 h at 60 mA
Averaged Dynamic Pressure	$3 \times 10^{-7}$ Pa at 60 mA
Averaged Static Pressure	$2 \times 10^{-8}$ Pa
Vacuum Pumps	TSP: 184, DIP: 56, SIP: 111*
Number of Insertion Devices	6 (In-vacuum Undulators: 5)

\*TSP: Titanium Sublimation Pump, SIP: Sputter Ion Pump

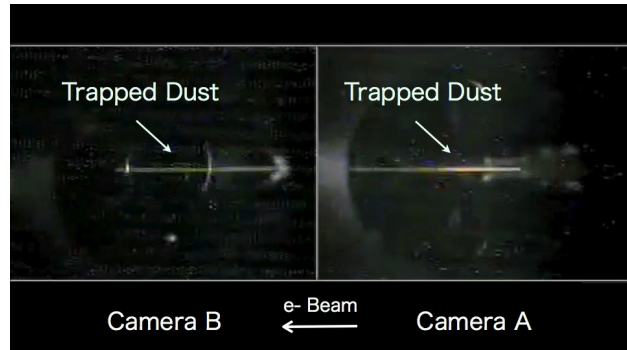


Figure 1: Image of trapped dust [2]. Luminous dust was detected simultaneously by two video cameras.

In these past experiments, trapped dust was observed only once during a dust event triggered by the mechanical movement of an electrode, while it was not observed during the numerous dust events triggered by electric discharges. This fact indicated that the visual observation required certain vital conditions. However, the image analysis also suggested that trapped dust of a lower temperature and smaller size could be visually observed by higher sensitive cameras. Therefore, we replaced the standard video cameras with supersensitive ones (KPC-EX500 with Sony EXview HAD CCD). The new cameras have a low lux sensitivity of 0.0003 lx @ F1.2, which is about three orders of magnitude lower than the previous ones.

<sup>#</sup>yasunori.tanimoto@kek.jp

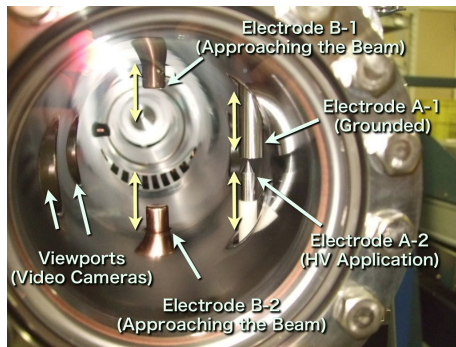


Figure 2: Interior view of the discharge device. Two pairs of electrodes are remotely controlled during the experiment. The electron beam passes from the front port to the back port. Inner diameter of the chamber is 100 mm.

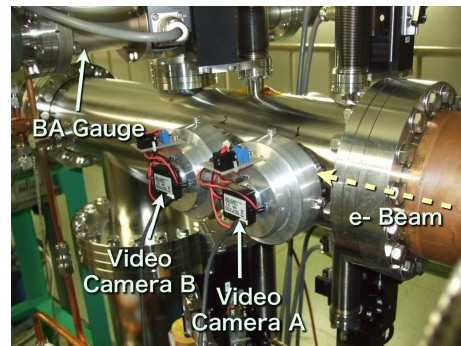


Figure 3: Exterior view of the discharge device. Cameras A and B detect dust particles as well as electric discharges at Electrodes A and B, respectively.

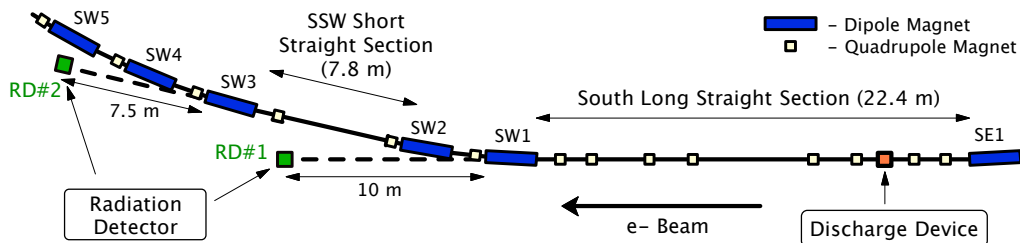


Figure 4: Layout of the experimental setup in the PF-AR [2].

## EXPERIMENTAL SETUP

The details of the experimental setup are described fully in Ref. [2]. In this paper, we briefly outline it.

Dust particles are intentionally produced by two kinds of electric discharges: one is caused by a DC HV application at Electrodes A, and the other is caused by beam-induced fields at grounded Electrodes B. The interior and exterior views of the discharge device are shown in Figs. 2 and 3, respectively.

Evidence of electric discharge is ensured by observing light emissions from the electrodes with video cameras, as well as by detecting an increase in vacuum pressure with a BAG. During the experiment using the supersensitive cameras, the BAG had to be switched off because the light from the BAG filament was too bright for the cameras.

Indirect evidence of dust trapping is obtained by the detection of bremsstrahlung gamma-rays from trapped dust by two radiation detectors (RDs). RD#1 is located on the extension of a long straight section where the discharge device is installed. RD#2 is located on the extension of the next short straight section, which is separated from the long straight section by two bending magnets. The layout of the experimental arrangement is shown in Fig. 4.

## EXPERIMENTAL RESULT

The dust-trapping experiments were conducted using supersensitive cameras. Intentional dust production was executed through two kinds of electric discharges. Figs

5A and 5B illustrate images of dust being ejected from Electrodes A and B, respectively, captured on the supersensitive cameras.

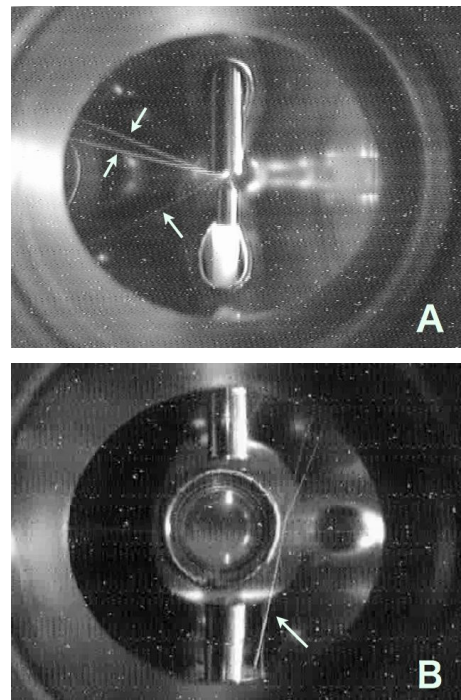


Figure 5: Dust particles produced by two kinds of intentional discharges. A: discharge generated by a high DC voltage of + 7.5 kV applied to Electrode A-2 (lower electrode); B: discharge generated by beam-induced RF fields in the slot of Electrode B-2 (lower electrode).

By using supersensitive cameras, luminous bodies were frequently observed in the electron beam orbit after the electric discharges. Light emissions from the luminous bodies were usually faint but recognizable. Whenever they were observed, the beam lifetime decreased and the radiation rate at RD#1 increased. In addition, there was a good proportional relation between the radiation rate at RD#1 and the beam loss rate. Therefore, we concluded that the luminous bodies observed in the electron beam orbit were the trapped dust particles.

In the experiments using Electrodes A, the trapped dust always moved fast, which was similar to the situation shown in Fig. 1, and disappeared within a second.

In the experiments using Electrodes B, on the other hand, the trapped dust had a tendency to stay in the same place, moving back and forward within a few tens of millimeters, for as long as we kept the positions of Electrodes B.

Fig. 6 shows an example of the trapped dust observed by Camera B, and Fig. 7 shows the experimental data obtained during this experiment. In this experiment, we moved Electrodes B-1 and B-2 symmetrically with respect to the beam orbit. When we changed the vertical distance between the tip of each electrode and the beam ( $D$ ) from 20 to 22 mm, the beam loss rate and the radiation rates at RD#1 and RD#2 increased. At the same time, the trapped dust was observed by Camera B. While the distance  $D$  was maintained between 17 and 23 mm for 40 minutes, the trapped dust continued to be observed. Upon some attempts to move Electrodes B by 1 or 2 mm, two dust particles trapped by the beam were simultaneously observed with Camera B. As soon as we started to withdraw Electrodes B to the initial position ( $D=50$  mm), the trapped dust disappeared and the beam lifetime recovered.

Thus, the supersensitive cameras were proved to detect dust-trapping events more effectively, and revealed that trapped dust particles behaved differently according to the position of Electrodes B. In order to investigate the reason behind the different behavior, we will improve the experimental setup.

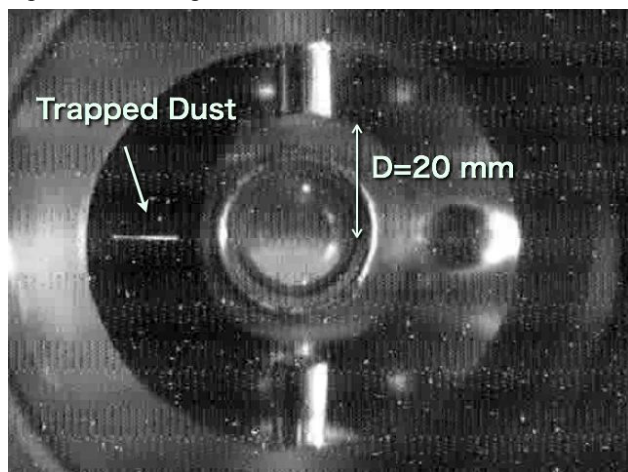


Figure 6: Image of trapped dust captured by supersensitive camera.

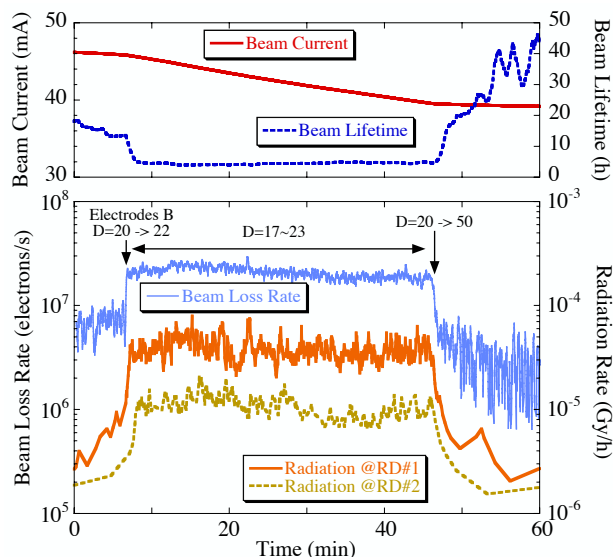


Figure 7: Experimental data obtained during the dust-trapping experiment using Electrodes B.

## FUTURE PLANS

We are planning to increase the number of cameras, which will enable us to observe the movement of the trapped dust over wider regions and from different angles. We are also planning to monitor dust movement with high-speed cameras. These observations will be helpful in investigating the dust-trapping mechanism.

In addition to continuing the visual observation of dust trapping, we will examine some operational conditions to remove trapped dust from electron beams by virtue of the good reproducibility of dust trapping. To examine the effect of a clearing electrode to which a DC voltage is applied [4, 5, 6], to vary the acceleration RF voltage [7], to oscillate the electron beam by a transverse kicker [8, 9], and to change the beam orbit by adding a DC bump, are candidates for future research.

## REFERENCES

- [1] Y. Tanimoto, T. Honda, T. Uchiyama, and T. Nogami, *AIP Conf. Proc. (Proc. 10th Int. Conf. on Synch. Radiat. Instrum., Melbourne, 2009)*, to be published.
- [2] Y. Tanimoto, T. Honda, and S. Sakanaka, *Phys. Rev. ST Accel. Beams* **12** (2009) 110702.
- [3] F. Zimmermann, PEP-II AP Note 8-94 (1994).
- [4] K. Huke et al., *IEEE Trans. Nucl. Sci.* **NS-30** (1983) 3130.
- [5] H. Saeki and T. Momose, *J. Vac. Sci. Technol. A* **18** (2000) 492.
- [6] F. Pedersen, A. Poncet, and L. Soby, *Proc. PAC '89*, p. 1786.
- [7] Q. Qin and Z. Y. Guo, *Proc. APAC '01*, p. 451.
- [8] U. Wienands, *Proc. PAC '01*, p. 597.
- [9] D. R. C. Kelly, *Proc. EPAC '96*, p. 442.